

A FLAsH-based FRET approach to determine G protein-coupled receptor activation in living cells

Carsten Hoffmann¹, Guido Gaietta², Moritz Bünemann¹, Stephen R Adams³, Silke Oberdorff-Maass¹, Björn Behr¹, Jean-Pierre Vilardaga¹, Roger Y Tsien³, Mark H Ellisman² & Martin J Lohse¹

Fluorescence resonance energy transfer (FRET) from cyan to yellow fluorescent proteins (CFP/YFP) is a well-established method to monitor protein-protein interactions or conformational changes of individual proteins. But protein functions can be perturbed by fusion of large tags such as CFP and YFP. Here we use G protein-coupled receptor (GPCR) activation in living cells as a model system to compare YFP with the small, membrane-permeant fluorescein derivative with two arsen-(III) substituents (fluorescein arsenical hairpin binder; FLAsH) targeted to a short tetracysteine sequence. Insertion of CFP and YFP into human adenosine A_{2A} receptors allowed us to use FRET to monitor receptor activation but eliminated coupling to adenylyl cyclase. The CFP/FLAsH-tetracysteine system gave fivefold greater agonist-induced FRET signals, similar kinetics (time constant of 66–88 ms) and perfectly normal downstream signaling. Similar results were obtained for the mouse α_{2A} -adrenergic receptor. Thus, FRET from CFP to FLAsH reports GPCR activation in living cells without disturbing receptor function and shows that the small size of the tetracysteine-biarsenical tag can be decisively advantageous.

In recent years, a large number of genetically encoded fluorescent sensors have been developed that measure protein-protein interactions or conformational changes of a protein of interest based on FRET¹. These systems have mostly used variants of the green fluorescent protein (GFP) from *Aequorea victoria*. A problem with GFP and its derivatives is their relatively large size and hence risk of altering the properties of the labeled protein(s). For example, in fusions, CFP and YFP have altered some properties of GPCRs². Agonist-induced activation of GPCRs is thought to cause a conformational rearrangement of their seven transmembrane α helices^{3,4}, most notably helices III and VI (refs. 3 and 5). Insertion of CFP into the third intracellular loop and fusion of YFP to the C terminus of a GPCR allows monitoring of agonist-induced activation, but impairs G protein coupling², as the third intracellular loop is a G protein coupling region^{6,7}.

Fluorescent probes for GPCR activation will be very useful for the study of the activation process and for drug screening⁸.

However, the pharmacological and signaling properties of the receptor should not be disturbed by the necessary modifications. Therefore, we set out to develop an alternative approach based on FLAsH, a small fluorescent probe that we have developed for labeling of proteins in intact cells^{9,10}. FLAsH is nonfluorescent by itself but becomes highly fluorescent when bound to a specific sequence consisting of at least six amino acids^{9,10}. The best sequence for FLAsH binding known so far is CCPGCC¹¹. FLAsH is much smaller than GFP (Fig. 1a), and therefore there is a much lower risk that FLAsH will disturb the overall structure of a protein.

Although FLAsH has been used for specific labeling of cellular proteins and for the study of long-term protein dynamics^{10,12}, no study has used FLAsH in combination with other fluorophores in dynamic FRET experiments. Here we report the use of FLAsH and CFP in dynamic FRET experiments using GPCR activation as a test system and demonstrate substantial improvements compared to the previously published CFP/YFP approach².

RESULTS

Generation of receptor constructs

We generated various receptor constructs based on the human A_{2A} adenosine receptor with modifications in different positions. CFP or the FLAsH-binding motif (CCPGCC) were introduced into the third intracellular loop of the receptor, and CFP or YFP were fused to its C terminus, respectively (Fig. 1b). Each receptor construct was fused with CFP at the same position of the C terminus. In the construct A_{2A}-CFP-Flash-C the sequence AEAAARECCPGCC_CCARA, which binds FLAsH with high affinity¹¹, was fused to the C terminus of CFP. In the construct A_{2A}-Flash3-CFP, the CCPGCC sequence was in the third intracellular loop.

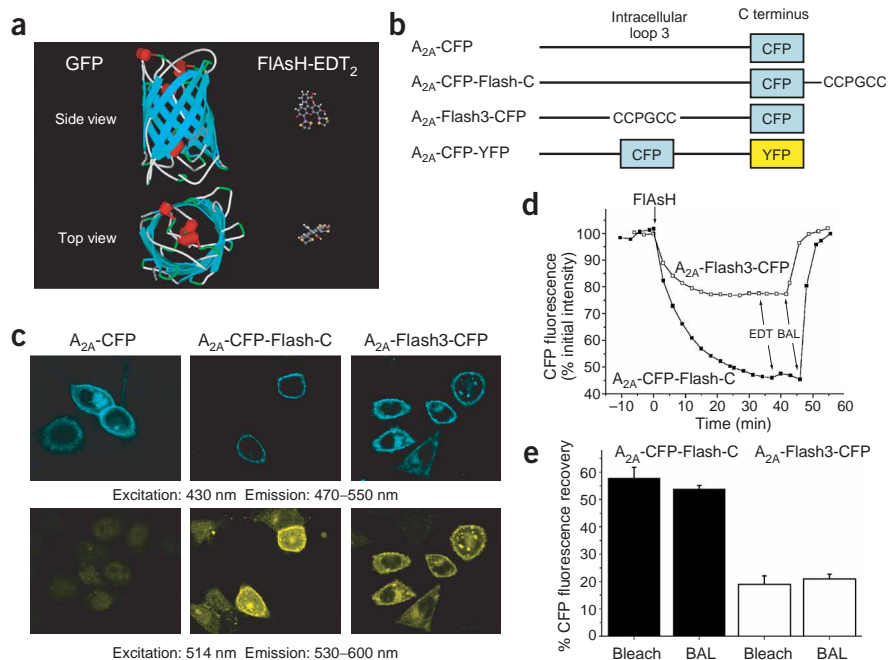
Specific labeling of receptor constructs with FLAsH

The specificity of FLAsH binding to the CCXXCC motif has been shown *in vitro*^{9,11} and *in vivo*^{10,12}. To demonstrate that FLAsH specifically binds to our receptor constructs, we transiently transfected HeLa cells with sequences encoding one of three different constructs (A_{2A}-CFP, A_{2A}-CFP-Flash-C and A_{2A}-Flash3-CFP) and incubated the cells with FLAsH. We excited the cells with two

¹Institute of Pharmacology and Toxicology, University of Würzburg, Versbacher Str. 9, D-97078 Würzburg, Germany. ²National Center of Microscopy and Imaging Research, Department of Neuroscience, and ³Department of Pharmacology, University of California, San Diego, 9500 Gilman Drive, La Jolla, California 92093, USA. Correspondence should be addressed to M.J.L. (lohse@toxi.uni-wuerzburg.de).

Figure 1 | Labeling of A_{2A} receptor constructs.

(a) Size comparison of GFP (backbone only) and FIAsh-EDT₂. (b) Schematic representation of receptor constructs. All constructs are variants of the human A_{2A} wild-type receptor and were modified as indicated either at the C terminus, the third intracellular loop, or both locations. (c) Confocal microscopy images of three different receptor constructs transiently expressed in HeLa cells and labeled with FIAsh. Top, CFP fluorescence. All receptor constructs were expressed at the cell surface. Bottom, FIAsh-fluorescence. All cells show dim yellow background fluorescence owing to nonspecifically bound FIAsh, but the cells expressing constructs containing the FIAsh binding motif (center and right) show a strong yellow fluorescence at the cell surface. (d) FRET between CFP and FIAsh in A_{2A} adenosine receptors. HEK-293 cells transiently transfected with the construct A_{2A} -CFP-Flash-C or A_{2A} -Flash3-CFP were incubated at the indicated time point with 500 nM FIAsh. Fluorescence intensity of CFP (450–515 nm) was measured every 3 min. We added 250 μ M EDT and 5 mM BAL as indicated by the arrows. (e) Comparison of FRET efficiency determined by fluorescence recovery after acceptor bleaching (Bleach) and after BAL treatment (BAL). Data are \pm s.e.m. of 9–12 cells from three separate experiments.



different wavelengths, one specific for CFP (430 nm) and the other specific for FIAsh (514 nm), and monitored them using a confocal microscope.

Images obtained after excitation of CFP at 430 nm showed expression of the three receptor constructs at the surface of HeLa cells (Fig. 1c, top). Images obtained after excitation at 514 nm demonstrated specific labeling with FIAsh of only the two receptor constructs containing the FIAsh binding motif (Fig. 1c, bottom). In contrast, cells expressing the construct A_{2A} -CFP that cannot specifically bind FIAsh showed only dim yellow background fluorescence, demonstrating that nonspecific FIAsh labeling was low and that CFP was not fluorescent when excited at 514 nm (Fig. 1c, bottom). A comparison of transfected (CFP-positive) and nontransfected (CFP-negative) cells demonstrated that nonspecific FIAsh labeling amounted to about one-fifth of the specific labeling (Fig. 1c, bottom). These data show that the insertion of the CCPGCC motif allowed specific labeling of the receptors with FIAsh.

FRET between FIAsh and CFP

To investigate whether FRET occurred between FIAsh and CFP, we mounted cells transfected with the construct encoding A_{2A} -CFP-Flash-C or A_{2A} -Flash3-CFP on a fluorescence microscope and incubated them with 500 nM FIAsh. Progressive labeling was monitored by short (100-ms, to minimize photobleaching) excitation pulses every 3 min. A time-dependent decrease in CFP fluorescence that reached a plateau after 20–40 min was observed for both constructs (Fig. 1d). Further increases in FIAsh concentration did not further decrease CFP fluorescence (data not shown), indicating that labeling was complete. Washing with 250 μ M 1,2-ethanedithiol (EDT) after attainment of equilibrium did not affect donor (CFP) fluorescence. But CFP fluorescence recovered

when the acceptor fluorescence was eliminated by stripping FIAsh from the tetracysteine using 5 mM 2,3-dimercapto-1-propanol (BAL), a vicinal dithiol with even higher affinity for arsenicals than EDT. BAL completely dequenched the CFP fluorescence (Fig. 1d). This experiment allowed us to estimate the FRET efficiency at $21 \pm 2\%$ for A_{2A} -Flash3-CFP and $54 \pm 3\%$ for A_{2A} -CFP-Flash-C (Fig. 1e).

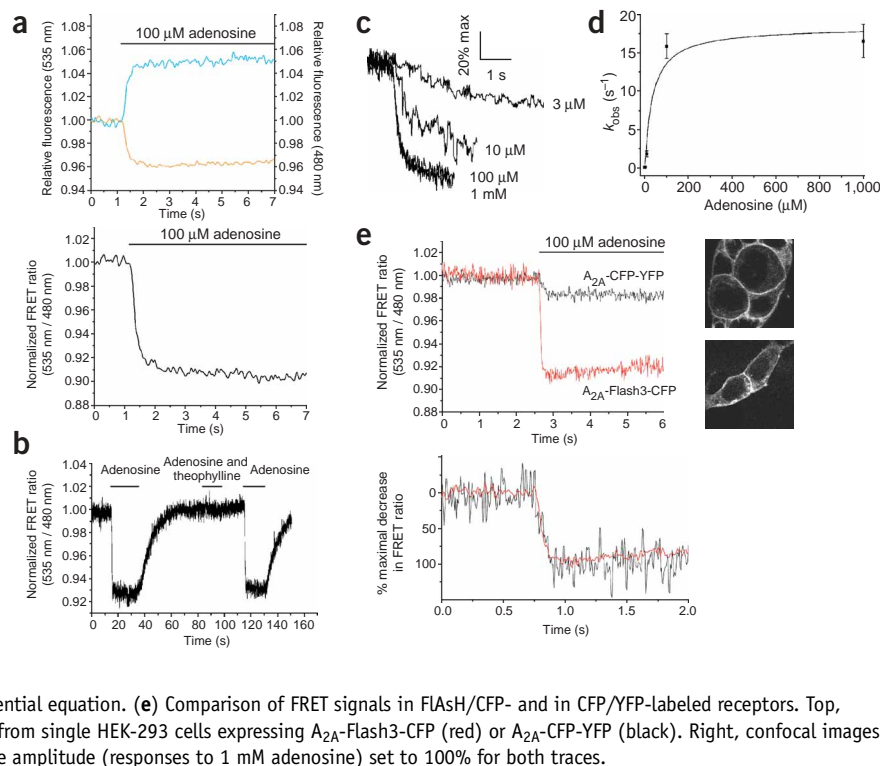
FRET efficiency was also measured by donor dequenching after acceptor photobleaching: we illuminated the FIAsh-labeled cells for 5 min at 514 nm to bleach FIAsh completely and measured fluorescence recovery of the donor fluorophore. The values obtained were quite similar to those determined with the BAL experiments: $19 \pm 3\%$ for A_{2A} -Flash3-CFP and $58 \pm 4\%$ for A_{2A} -CFP-Flash-C (Fig. 1e).

Agonist-dependent changes in FRET signals

We then investigated whether the FRET signal obtained with A_{2A} -Flash3-CFP was sensitive to agonist stimulation. HEK-293 cells transiently expressing this construct were labeled with FIAsh and then stimulated by superfusion with the agonist adenosine. This led to a symmetrical decrease of the FIAsh emission and increase of the CFP emission and thus to a rapid loss of FRET, indicated by $\sim 10\%$ decrease in the 535 nm/480 nm FRET ratio (Fig. 2a). The loss of FRET is compatible with the hypothesis that activation would lead to an increased distance between the third intracellular loop and the C terminus of GPCRs² as predicted by computer simulations with the α_{1B} -adrenergic receptor⁷.

In contrast to A_{2A} -Flash3-CFP, the construct A_{2A} -CFP-Flash-C that has both fluorophores at the C terminus did not change fluorescence upon agonist stimulation (data not shown). Coexpression of A_{2A} -CFP and A_{2A} -Flash3 (carrying only the Flash motif in the third intracellular loop but lacking the CFP) showed no

Figure 2 | Adenosine-induced changes in FRET in FLAsH/CFP-labeled A_{2A} receptors (A_{2A} -Flash3-CFP). (a) Changes in the relative fluorescence of CFP or FLAsH (top) and corresponding FRET ratio (bottom) in response to 100 μ M adenosine from a single HEK-293 cell expressing the construct A_{2A} -Flash3-CFP. Initial values of relative fluorescence (top) or of the normalized FRET ratio (bottom) were set to one. The recording is representative of a large number of independent experiments. (b) Changes in the FRET ratio of A_{2A} -Flash3-CFP expressed in HEK-293 cells upon agonist stimulation and blockade by an antagonist. Superfusion was done with buffer, with (or without) 10 μ M adenosine with or without 500 μ M theophylline. (Representative experiment, $n = 3$). (c) Kinetics of adenosine-mediated change in the FRET ratio. The change in the normalized FRET ratio in response to different concentrations of the agonist adenosine measured in single cells expressing A_{2A} -Flash3-CFP. The recordings are expressed as % of the maximal response achieved with 1 mM adenosine (representative experiment, $n = 4$). (d) Relationship between the adenosine concentration and k_{obs} , the apparent rate constant of the change in the FRET ratio. k_{obs} values were obtained from fitting the kinetic data to a monoexponential equation. (e) Comparison of FRET signals in FLAsH/CFP- and in CFP/YFP-labeled receptors. Top, normalized FRET ratios in response to 1 mM adenosine from single HEK-293 cells expressing A_{2A} -Flash3-CFP (red) or A_{2A} -CFP-YFP (black). Right, confocal images of the respective receptors. Bottom, same data with the amplitude (responses to 1 mM adenosine) set to 100% for both traces.



FRET in the absence or presence of 100 μ M adenosine (data not shown). These control experiments indicate that it is unlikely that the observed signals resulted from intermolecular FRET in receptor dimers. But it should be noted that the intramolecular nature of this signal does not exclude the presence of receptor dimers.

The agonist-induced change in the FRET signal of the A_{2A} -Flash3-CFP construct was blocked by an antagonist, theophylline. In consecutive stimulations of the same cell with 10 μ M adenosine, a robust signal was obtained with adenosine alone, whereas no response was seen in the presence of 500 μ M theophylline (Fig. 2b). Theophylline alone had no effect, and in accordance with the pattern expected for competitive antagonism, raising the adenosine concentration to 100 μ M partially reversed the theophylline block (data not shown).

Time-resolved recordings of the FRET signals from single cells after activation with adenosine allowed the analysis of the activation switch kinetics (Fig. 2c,d). Under all conditions, the decrease of the FRET ratio (535 nm/480 nm) followed a monoexponential time course. Increasing concentrations of adenosine resulted in faster time courses of the signals, until at higher concentrations the rate constants (k_{obs}) reached a maximum, suggesting that a step other than agonist binding became rate limiting. This limit is not due to technical limitations of the system, which allows complete solution exchange in < 10 ms, and therefore most likely represents (or at least includes) the agonist-mediated conformational switch of the receptors. The maximal k_{obs} values of 15–20 sec^{-1} indicate a time constant required for receptor activation of 50–70 ms.

Comparison of FLAsH/CFP with CFP/YFP-modified receptors

To compare the new labeling approach to that using CFP and YFP, we created an adenosine receptor (A_{2A} -CFP-YFP), in which CFP

was inserted in the third intracellular loop at the position of the FLAsH-binding motif in A_{2A} -Flash3-CFP, and YFP was at the C terminus instead of CFP (Fig. 1b).

A direct comparison of the two FRET approaches shows that the amplitude of the signal for the FLAsH/CFP-modified receptor was five times higher than that of the CFP/YFP-modified receptor (Fig. 2e). But the time constant of receptor activation was not substantially different for the two approaches. When the two FRET signals were normalized with respect to the signal amplitude (Fig. 2e, bottom), the FLAsH/CFP-based approach gave a time constant of 66 ± 8 ms ($n = 7$), whereas the CFP/YFP-based approach gave a value of 88 ± 18 ms ($n = 5$). These values are close to those previously reported for the CFP/YFP-labeled α_{2A} -adrenergic receptor (~ 50 ms) but are much faster than for the

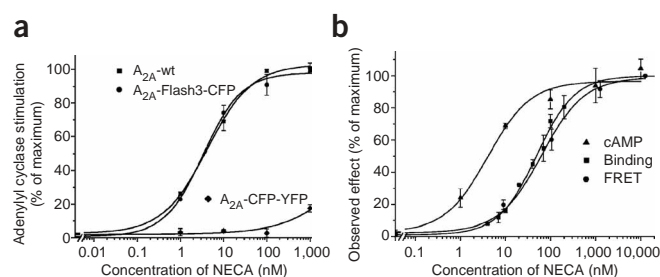
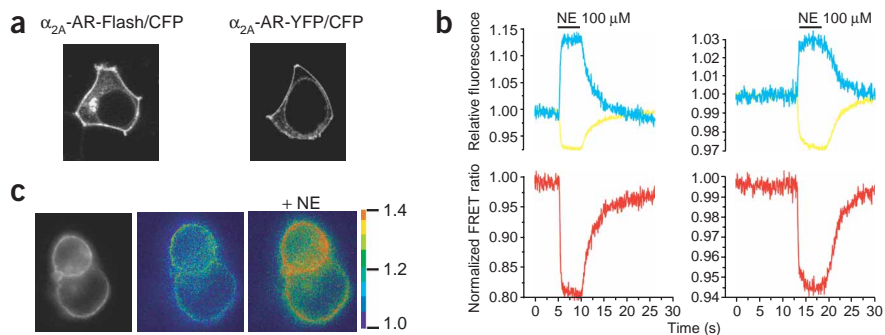


Figure 3 | Pharmacological properties of the A_{2A} receptor constructs. (a) Stimulation of adenylyl cyclase activity by NECA in cell membranes from HEK cells expressing A_{2A} wild-type receptors (squares), A_{2A} -Flash3-CFP (circles), or A_{2A} -CFP-YFP (diamonds). Data are \pm s.e.m. ($n = 3$). (b) Comparison of NECA-binding (squares), NECA-induced changes in FRET (circles) and NECA-induced adenylyl cyclase stimulation (triangles) for A_{2A} -Flash3-CFP. All data are given as percent of the response induced by 1 mM NECA. Data are \pm s.e.m. ($n = 3$ –4).

Figure 4 | Application of the FIAsh/CFP approach to the α_{2A} -adrenergic receptor. **(a)** Confocal pictures show the cellular expression of the α_{2A} -AR-Flash/CFP and α_{2A} -AR-YFP/CFP in transiently transfected HEK-293 cells. Both receptor constructs exhibit predominant localization to the plasma membrane. **(b)** Changes in the fluorescence (top) of CFP and FIAsh (left) or CFP and YFP (right), respectively and corresponding FRET-ratio (bottom) in response to 100 μ M norepinephrine were recorded from a single HEK-293 cell expressing α_{2A} -AR-Flash/CFP or α_{2A} -AR-YFP/CFP. Initial values of relative fluorescence (top; blue, 480 nm and yellow, 535 nm) or of the normalized FRET ratio (bottom; red, 535 nm/480 nm) were set to one. The recording is representative of a large number of independent experiments. **(c)** FRET imaging of receptor activation in HEK-293 cell transiently transfected with α_{2A} -AR-Flash/CFP. The left panel shows fluorescence emission of the cells upon excitation at 430 nm. The next two panels show the FRET ratio presented as a false-color image (480 nm/535 nm) before and after stimulation with 100 μ M norepinephrine. The scale bar on the right indicates the false-color scale of the ratios.



PTH receptor studied by the same approach (~ 1 sec)². The signal-to-noise ratio of the FIAsh/CFP-based approach is substantially better when compared to the CFP/YFP-based approach (**Fig. 2e**).

Pharmacological characterization of receptor constructs

To investigate whether the insertion of the CCPGCC motif or GFP variants into the receptor affect the receptor's binding or signaling properties, the wild-type A_{2A} receptor, A_{2A} -Flash3-CFP and A_{2A} -CFP-YFP were each transiently expressed in COS-1 cells. All three receptors were expressed at comparable levels varying from 8 to 12 pmol/mg protein and bound the agonist radioligand [³H]NECA with affinities of 52 ± 9 , 63 ± 11 and 63 ± 18 nM, respectively (data not shown).

The constructs were analyzed for their signaling properties by determination of adenylyl cyclase activation upon receptor stimulation with NECA (**Fig. 3a**). The activation curves for the wild-type receptor and A_{2A} -Flash3-CFP were superimposable, suggesting that the G protein coupling and signaling properties of the receptor were not affected by these labels. In marked contrast, the receptor construct A_{2A} -CFP-YFP mediated almost no adenylyl cyclase stimulation even at high agonist concentrations.

The NECA-binding and FRET signal curves of A_{2A} -Flash3-CFP were superimposable, whereas—owing to signal amplification—the adenylyl cyclase activation curve was shifted to lower concentrations by one order of magnitude (**Fig. 3b**). This illustrates that the FRET signal faithfully records the agonist-occupied active state of the receptor rather than a downstream-mediated effect.

FIAsh/CFP labeling of α_{2A} -adrenergic receptors

To investigate whether this FIAsh/CFP approach can be applied to other systems, we constructed an α_{2A} -adrenergic Flash/CFP receptor (α_{2A} -AR-Flash/CFP) containing the CCPGCC motif instead of the YFP in the previously published α_{2A} -YFP/CFP receptor². Confocal images (**Fig. 4a**) showed that even in transiently transfected HEK-293 cells both receptor constructs are primarily expressed at the plasma membrane. A typical trace of the agonist-induced change in the FRET signal is shown in **Figure 4b**. Upon superfusion with norepinephrine, the change in the FRET signal was again more than threefold greater for the FIAsh/CFP construct than for the CFP/YFP receptor and amounted to up to a 20% change. This change in signal amplitude was large enough for

imaging of receptor activation in real time. We transfected HEK-293 cells with α_{2A} -AR-Flash/CFP, labeled them with FIAsh and recorded FRET images with a dual-emission CCD camera. Upon superfusion with norepinephrine, the cells showed a marked change in fluorescence ratio (**Fig. 4c**). The bar on the right shows the false-color scale of the corrected CFP/FIAsh emission. Note that in this experiment the CFP/FIAsh ratio is such that addition of agonist increases the ratio. A movie of the experiment reveals the temporal as well as the spatial resolution of our FIAsh/CFP imaging technique (**Supplementary Video 1** online).

DISCUSSION

The recently described direct monitoring of receptor activation with optical techniques opens new dimensions of temporal and spatial information on the activation of GPCRs^{2,8}. But the technique based on the fusion of two GFP variants to the receptor has drawbacks owing to the large size of the fluorescent markers, which can lead to alterations in the pharmacological and signaling properties of the receptors.

Therefore, we have developed a modification of this system that replaces the fluorescent protein in the third intracellular loop of the receptor with tetracysteine-FIAsh and uses CFP at the C terminus as the fluorescence donor. This approach is the first report of dynamic FRET using FIAsh in combination with CFP to monitor conformational changes in a protein and illustrates the potential of this small fluorescent marker to label defined proteins in an intact cell. Its much smaller size compared to GFP resulted in preservation of the pharmacological properties of the A_{2A} receptor with respect both to agonist binding and to agonist-induced cAMP signaling. This is remarkable because the insertion of a fluorescent protein at the same site in this receptor (that is, the third intracellular loop) virtually abolished the signaling capacity of the receptor.

In addition to preserving the receptor's pharmacological properties, the FIAsh approach also resulted in much larger agonist-induced changes in FRET, both in the A_{2A} -adenosine and the α_{2A} -adrenergic receptor (**Figs. 2e** and **4b**). This increased signaling amplitude appeared to be a true sensing property of the FIAsh-labeled receptors, as both the FIAsh/CFP- and CFP/YFP-labeled receptors were primarily targeted to the cell surface and thus were available for agonist activation. A possible explanation is the relative distance and orientation of the two fluorophores: because

FLAsH directly binds to the CCPGCC motif, it is located directly at the third intracellular loop of the receptor, whereas in the case of the fluorescent proteins the fluorophore is located inside the β barrel ~ 10 – 15 Å away from the site of attachment in the third intracellular loop. In addition, the attachment of FLAsH at its binding site may be less flexible than that of YFP and, therefore, FLAsH may more faithfully report the conformational change.

It might be assumed that the presence of FLAsH instead of YFP would permit the receptor to switch faster in response to agonists, as the large additional protein moiety might restrain the receptor's movement. This, however, was not the case. There are two mutually nonexclusive explanations for this observation. The actual conformational change makes up only part of the k_{obs} measured for receptor activation. For example, ligand diffusion, binding to the relevant site within the receptor and the fact that we observed a multitude of receptors at the cell surface rather than a single one might all contribute to apparent switch times that are longer than the actual conformational change. Alternatively, the presence of a 27-kDa fluorescent protein in the third intracellular loop does not limit the speed of the conformational change within the receptor protein. Based on the measured translational and rotational diffusion behavior of GFP in cytoplasm¹³, one can calculate that GFP by itself can undergo major rotations or a 2.5-nm lateral diffusion in only tens of nanoseconds, some six orders of magnitude less than the 66–88 ms observed for the receptor switch. Thus, a fused GFP mutant can be completely nondisruptive with respect to intrinsic conformational kinetics of the receptor, whereas it severely obstructs interaction with downstream effectors.

The improved agonist-induced FRET signal for the A_{2A} -Flash3-CFP construct enabled us to compare this signal with radioligand binding and cAMP production induced by the same ligand. The data obtained for the FRET signal are almost superimposable with those from radioligand binding (Fig. 3b). This would be expected if binding of an agonist directly led to a conformational change in the receptor. Thus, only agonist-occupied receptors should change their relative FRET ratio and, therefore, the signal should follow binding of the ligand. The leftward shift for the cAMP accumulation (Fig. 3b) relative to radioligand binding and the FRET signal probably is due to a receptor reserve: not all receptors need to be activated to generate a full cAMP signal. Furthermore, the antagonist theophylline blocked the agonist-induced change in the FRET signal (Fig. 2b) and did not induce a signal by itself (data not shown). This suggests that the FRET signal reflects agonist-induced receptor activation. An interesting feature of the FLAsH-labeled receptors is the greater amplitude of the agonist-induced FRET signal. This should allow more detailed analysis of the properties of compounds that only partially activate receptors, as seen for the β_2 -adrenergic receptor using purified receptors and a different fluorescence labeling system¹⁴ and the α_{2A} -AR-CFP/YFP system². In particular, it will be interesting to determine whether the existence of several distinct agonist-induced states, which have recently been determined for the β_2 -adrenergic receptor^{14,15}, also holds for other GPCRs, and to delineate whether FRET signals can be used to distinguish between these states. This potential of our new technology will have to be thoroughly investigated in the future. Another potential application of this technique is outlined in Figure 4c. The amplitude of the signal change for the α_{2A} -AR-Flash/CFP construct was large

enough to use the receptor construct for imaging of receptor activation in real time. This experiment indicates that this technique can be applied to visualize receptor activation in other relevant physiological models.

Taken together, the use of FLAsH as a label in conjunction with CFP improves detection of GPCR activation at the single cell level. We believe that the use of this approach will substantially advance both the analysis of the mechanisms of receptor activation and the use of optical methods in ligand screening. Although the small size of the tetracysteine-biarsenical tagging system has long been theoretically attractive, this example is the first direct demonstration of a major reduction in perturbation of host protein function.

METHODS

Molecular biology and cell culture. Site-directed mutagenesis was performed on the human adenosine A_{2A} receptor cDNA (GenBank entry X68486). The cDNAs encoding the enhanced CFP and YFP were fused to the receptor cDNA such that the fluorescent protein would follow position Gly340 or Val323 of the receptor's C terminus. CFP or the CCPGCC motif were also substituted for the sequence from Pro215 to Arg220 in the third intracellular loop of the receptor. A similar α_{2A} -AR-Flash/CFP construct was obtained by fusion at position Val461 with CFP, and the CCPGCC motif was inserted in the third intracellular loop between Ala250 and Ser371. Constructions were performed by PCR of the cDNA and verified by sequencing. Receptor cDNAs were cloned into pcDNA3 (Invitrogen) for expression in HeLa, HEK-293 and COS-1 cells. COS-1 cells were transfected using DEAE-Dextran¹⁶, and Effectene (Qiagen) was used for HEK-293 and HeLa cells. For fluorescence measurements, cells were split 24 h after transfection and seeded on polylysine-coated coverslips that were placed in six-well plates. Cells were kept in culture for an additional 24 h. For live-labeling experiments and the determination of FRET efficiency, cells were cultured on 3-cm MatTek dishes (MatTek Corporation).

FLAsH labeling. The labeling was done essentially as described¹⁰. Transfected cells grown on coverslips or MatTek dishes were washed twice with phenol red-free Hank's balanced salt solution containing 1g/l glucose (HBSS; Invitrogen) and then incubated at 37 °C for 1 h with 500 nM or 1 μ M FLAsH suspended in HBSS containing 12.5 μ M EDT. Next, cells were rinsed twice with HBSS, incubated for 10 min with HBSS containing 250 μ M EDT and again rinsed twice with HBSS to reduce nonspecific labeling. FLAsH is commercially available from Invitrogen as Lumino Green.

Confocal microscopy. Confocal microscopy was performed using a Leica TCS SP2 system with an Attofluor holder (Molecular Probes). FLAsH was excited with the 514-nm line of an argon laser, and images were taken with a 63 \times objective using the factory settings for YFP fluorescence (530–600 nm). CFP was excited at 430 nm with a frequency-doubled diode laser (Leica) and images were taken using the factory settings for CFP fluorescence (470–550 nm).

Live labeling and determination of FRET efficiency. HEK-293 cells cultured in 3-cm MatTek dishes were transiently transfected as described above. After 24 h, cells were washed twice with phenol red-free HBSS and maintained in 1.9 ml HBSS buffer. MatTek

dishes were mounted on a Zeiss Axiovert135 inverted fluorescence microscope and measured using MetaFluor software. The following excitation/dichroic/emission filters were used: for CFP, 420 ± 20 nm/450 nm/475 ± 40 nm; for FAsH, 495 ± 10 nm/505 nm/535 ± 25 nm; and for FRET between CFP and FAsH, 420 ± 20 nm/450 nm/535 ± 25 nm. Light pulses were of 100-ms duration. To monitor labeling, regions of interest were defined and a time drive was set to take pictures with the above settings every 3 min. After 10 min, 100 µl of a freshly prepared mix of FAsH dye and EDT was added to a final concentration of 500 nM FAsH and 12.5 µM EDT. Fluorescence emission was monitored until a plateau was reached. Next, the incubation mixture was aspirated carefully, ensuring that no movement of the specimen occurred; cells were incubated with HBSS supplemented with 250 µM EDT; and fluorescence emission was monitored every 3 min. After 10 min, the incubation mixture was carefully aspirated and cells were incubated with HBSS. FRET between CFP and FAsH was then quantified by two different methods: (i) treatment with BAL to compete for FAsH binding and (ii) donor dequenching after acceptor photobleaching (5-min illumination at 495 nm).

Fluorescence measurements and cell imaging. Fluorescence microscopy was performed as described^{2,17}. Cells labeled as described above were washed with HBSS and maintained in buffer A (140 mM NaCl, 5 mM KCl, 2 mM CaCl₂, 1 mM MgCl₂, 10 mM HEPES, pH 7.3) at room temperature. Coverslips were mounted on an Atofuo holder and placed on a Zeiss Axiovert135 inverted microscope equipped with an oil immersion 63× objective and a dual emission photometric system (Till Photonics). Samples were excited with light from a polychrome IV (Till Photonics). To minimize photobleaching, the illumination time was set to 5 ms, applied with a frequency between 1 and 100 Hz depending on agonist concentration. The fluorescence signal was recorded from the entire cell. FRET was monitored as the emission ratio of FAsH to CFP, F_{535}/F_{480} (emission intensities at 535 ± 15 nm and 480 ± 20 nm; beam splitter DCLP 505 nm) upon excitation at 436 ± 10 nm (beam splitter DCLP 460 nm). The emission ratio was corrected for the spillover of CFP into the 535 nm channel (spillover of FAsH into the 480 nm channel was negligible) to give a corrected ratio (F_{535}^*/F_{480}^*). The FAsH emission upon excitation at 480 nm was recorded at the beginning of each experiment to subtract direct excitation of FAsH (FAsH emission at 436 nm excitation divided by FAsH emission at 480 nm excitation was 0.06). To determine agonist-induced changes in FRET, cells were continuously superfused with buffer A, and agonist was applied using a computer-assisted solenoid valve-controlled rapid superfusion device ALA-VM8 (ALA Scientific Instruments; solution exchange 5–10 ms). Signals detected by avalanche photodiodes were digitized using an AD converter (Digidata1322A, Axon Instruments) and stored on PC using Clampex 8.1 software (Axon Instruments). The decrease in FRET ratio (r) was fitted to the equation $r(t) = A \times e^{-t/\tau}$, where τ is the time constant (s) and A is the magnitude of the signal. When necessary for calculating τ , agonist-independent changes in FRET owing to photobleaching were subtracted. The imaging data were recorded as previously described¹⁸. Data were analyzed with MetaMorph 5.0 (Visitron Systems).

Pharmacology. Membrane preparation, ligand binding and determination of adenylyl cyclase activity were performed as previously described¹⁹. Saturation and competition binding studies were analyzed with the program Origin (OriginLab Corporation) to calculate K_D and K_i values.

Note: Supplementary information is available on the Nature Methods website.

ACKNOWLEDGMENTS

This work was supported by the Deutsche Forschungsgemeinschaft (Leibniz award to M.J.L. and grant HO 2357/1-1 to C.H.), a Bavaria California Technology Center (BaCaTeC) grant to C.H., a Fonds der Chemischen Industrie grant to M.J.L. and US National Institutes of Health grant P41RR004050 to M.H.E.

COMPETING INTERESTS STATEMENT

The authors declare competing financial interests (see the *Nature Methods* website for details).

Received 14 October 2004; accepted 26 January 2005

Published online at <http://www.nature.com/naturemethods/>

- Miyawaki, A. Visualization of the spatial and temporal dynamics of intracellular signaling. *Dev. Cell* **4**, 295–305 (2003).
- Vilardaga, J.P., Bünemann, M., Krasel, C., Castro, M. & Lohse, M.J. Measurement of the millisecond activation switch of G protein-coupled receptors in living cells. *Nat. Biotechnol.* **21**, 807–812 (2003).
- Gether, U. Uncovering molecular mechanisms involved in activation of G protein-coupled receptors. *Endocr. Rev.* **21**, 90–113 (2000).
- Pierce, K.L., Premont, R.T. & Lefkowitz, R.J. Seven-transmembrane receptors. *Nat. Rev. Mol. Cell Biol.* **3**, 639–650 (2002).
- Bissanz, C. Conformational changes of G protein-coupled receptors during their activation by agonist binding. *J. Recept. Signal Transduct. Res.* **23**, 123–153 (2003).
- Wess, J. G-protein-coupled receptors: molecular mechanisms involved in receptor activation and selectivity of G-protein recognition. *FASEB J.* **11**, 346–354 (1997).
- Greasley, P.J. *et al.* Mutational and computational analysis of the alpha(1b)-adrenergic receptor. Involvement of basic and hydrophobic residues in receptor activation and G protein coupling. *J. Biol. Chem.* **276**, 46485–46494 (2001).
- Milligan, G. Applications of bioluminescence- and fluorescence resonance energy transfer to drug discovery at G protein-coupled receptors. *Eur. J. Pharm. Sci.* **21**, 397–405 (2004).
- Griffin, B.A., Adams, S.R. & Tsien, R.Y. Specific covalent labeling of recombinant protein molecules inside live cells. *Science* **281**, 269–272 (1998).
- Gaietta, G. *et al.* Multicolor and electron microscopic imaging of connexin trafficking. *Science* **296**, 503–507 (2002).
- Adams, S.R. *et al.* New biarsenical ligands and tetracysteine motifs for protein labeling in vitro and in vivo: synthesis and biological applications. *J. Am. Chem. Soc.* **124**, 6063–6076 (2002).
- Ju, W. *et al.* Activity-dependent regulation of dendritic synthesis and trafficking of AMPA receptors. *Nat. Neurosci.* **7**, 244–253 (2004).
- Swaminathan, R., Hoang, C.P. & Verkman, A.S. Photobleaching recovery and anisotropy decay of green fluorescent protein GFP-S65T in solution and cells: cytoplasmic viscosity probed by green fluorescent protein translational and rotational diffusion. *Biophys. J.* **72**, 1900–1907 (1997).
- Swaminath, G. *et al.* Sequential binding of agonists to the β_2 adrenoceptor. Kinetic evidence for intermediate conformational states. *J. Biol. Chem.* **279**, 686–691 (2004).
- Liapakis, G., Chan, W.C., Papadokostaki, M. & Javitch, J.A. Synergistic contributions of the functional groups of epinephrine to its affinity and efficacy at the beta2 adrenergic receptor. *Mol. Pharmacol.* **65**, 1181–1190 (2004).
- Cullen, B.R. Use of eukaryotic expression technology in the functional analysis of cloned genes. *Methods Enzymol.* **152**, 684–704 (1987).
- Bünemann, M., Frank, M. & Lohse, M.J. Gi protein activation in intact cells involves subunit rearrangement rather than dissociation. *Proc. Natl. Acad. Sci. USA* **100**, 16077–16082 (2003).
- Nikolaev, V.O., Bünemann, M., Hein, L., Hannawacker, A. & Lohse, M.J. Novel single chain cAMP sensors for receptor-induced signal propagation. *J. Biol. Chem.* **279**, 37215–37218 (2004).
- Klotz, K.N. *et al.* Comparative pharmacology of human adenosine receptor subtypes—characterization of stably transfected receptors in CHO cells. *Naunyn Schmiedeberg Arch. Pharmacol.* **357**, 1–9 (1998).